Journal of Materials Chemistry C

Full color carbon dots through surface engineering for constructing white light-emitting diodes

Journal:	*Journal of Materials Chemistry C*
Manuscript ID	TC-COM-01-2019-000274
Article Type:	Communication
Date Submitted by the Author:	15-Jan-2019

Complete List of Authors:	Cai, Wei; China University of Petroleum Beijing Zhang, Ting; General Hospital of Chinese People's Liberation Army, Department of Orthopaedic Xu, Meng; General Hospital of Chinese People's Liberation Army Zhang, Miaoran; China University of Petroleum (Beijing), Institute of New Energy Guo, Yongjian; Beijing University of Chemical Technology Zhang, Lipeng; University of Tennessee, Materials Science and Engineering Street, Jason ; Mississippi State University, Department of Sustainable Bioproducts Ong, Wee-Jun; Xiamen University Malaysia, School of Energy and Chemical Engineering; Xiamen University, College of Chemistry and Chemical Engineering Xu, Quan; China University of Petroleum (Beijing), Institute of New Energy

Journal Name

ARTICLE

Full color carbon dots through surface engineering for constructing white light-emitting diodes

Received 00th January 20xx,
Accepted 00th January 20xx

DOI: 10.1039/x0xx00000x

www.rsc.org/

Wei Cai,†[a] Ting Zhang,†[b] Meng Xu,[b] Miaoran Zhang,[a] Yongjian Guo,[c] Lipeng Zhang,*[c] Jason Street,[d] Wee-Jun Ong,*[e,f] Quan Xu*[a]

White light-emitting diodes (WLEDs) devices are replacing the filament lamp and they can provide a light close to the natural sunlight, which have thus drawn considerable attention in these recent years. It remains a scientific challenge to develop WLEDs using environmentally friendly, easy-to-process and cost-effective phosphors. Here we synthesized blue-, green- and red-carbon dots (denoted as B-, G- and R-CDs) by a facile solvothermal method with high dispersity both in aqueous and organic solvent. The quantum yield (QY) of the R-CDs achieved up to 24.7%. These CDs can be easily dissolved in polyvinylpyrrolidone (PVP) colloid, leading to the production of ultraviolet (UV)-excited LED devices to avoid the retinal damage caused by blue ray excitation. The fluorescence emission of the WLED has a wide band, covering the whole visible light region. Importantly, the influence of doping that gives rise to the change of emissive colors has been elucidated by X-ray photoelectron spectroscopy (XPS) combined with a computation method in order to provide a systematic controllable tuning on the functionalization of CDs. As such, WLEDs were demonstrated with color coordinates of (0.33, 0.33), a color temperature of 5612 K in the CIE chromaticity diagram with good anti-photobleaching and a color rendering index (CRI) of 89.

Introduction

Carbon dots (CDs), as a new growing member of the carbon material family, have broadened the application of carbon-based materials in bioimaging,[1] catalysis,[2] energy storage,[3-4] environmental monitoring[5] and photoelectric conversion[6] due to the remarkable tuneable fluorescence, good photoelectric properties and biocompatibility.[7-9] Among the previous studies involving CDs, multi-color emission has been one of the most attractive properties for diverse applications.

In particular, multi-color photoluminescent materials have potential applications for light-emitting diodes (LEDs).[10-11] Conventional multi-color emissive materials have been explored in the past several decades, including not only inorganic materials like semiconductor quantum dots (QDs) and rare-earth based nanoparticles, but also organic fluorescent dyes and molecular nanomaterials.[12-16] However, the existing problems of the multi-color emissive materials encompass high toxicity, poor emission QY, instability due to photobleaching and water-insolubility, which have precluded for niche applications. As such, this dictates a pressing requirement for a green substitution. Recently, CDs with multi-color emissions have been successfully synthesized and applied on LED devices, which display high QY, tuneable wavelengths and narrow emission bands.[17-21] The distinctive carbon-base structure of metal-free CDs and excellent optical properties endow them an appealing candidate for LED devices, of which multiple colors can be applied for white light-emitting diodes (WLEDs).[22-26]

To develop practical applications concerning the use of CDs in WLEDs, one of the most crucial parts is to improve the QY of red emissive CDs (R-CDs), which have not been explored as extensively as other emissive CDs thus far. Most R-CDs recorded QYs of less than 10%,[17] and lately reached about 20% with the continuous development.[18, 27] The most common WLEDs that generate white light depend on a chip which emits blue light, which is associated with layers of fluorescent materials to produce long wavelengths. However, the present blue LED chip used for producing this

[a] State Key Laboratory of Heavy Oil Processing, China University of Petroleum-Beijing, 102249, China. *E-mail: xuquan@cup.edu.cn
[b] Training Division of the Medical Administration Department, Department of Orthopaedic, General Hospital of Chinese People's Liberation Army, 100853 Beijing, China
[c] College of Energy, Beijing University of Chemical Technology, Beijing, 100029, China. *E-mail: zhanglipeng2011@gmail.com
[d] Department of Sustainable Bioproducts, Mississippi State University, Starkville 39762, United States
[e] School of Energy and Chemical Engineering, Xiamen University Malaysia, Selangor Darul Ehsan 43900, Malaysia. *E-mail: ongweejun@gmail.com; weejun.ong@xmu.edu.my
[f] College of Chemistry and Chemical Engineering, Xiamen University, Xiamen 361005, China
† Wei Cai and Ting Zhang contribute equally to this work

white light can result in retinal damage.[28] Thus, reducing the harmless brought by blue excitation is another important component to optimize the WLED devices. UV-excited LED chips are desired to excite a broad white emission to avoid phototoxicity to human eyes from the blue LED chip.[29]

Surface functionalization/passivation with small organic molecules, polymers and doping with non-carbon elements (e.g. B, N, P, S) and sometimes metal elements (e.g. Zn, Ti, Mn) are typical in the preparation of CDs in the efforts to improve the photoluminescence (PL) property, water solubility and optical properties.[30-35] Herein, we employed p-phenylenediamine as monomer of cyclization with different modifying agents (such as amino acetic acid) to synthesize blue, green, and red emissive CDs using a facile one-pot solvothermal method. The QY of the R-CDs achieved up to 24.7% (Table S1). Due to the well-dissolved CDs in polyvinylpyrrolidone (PVP), we have fabricated CDs/PVP composites for LEDs, as well as the WLEDs with a Commission on Illumination (CIE) coordinate (0.33, 0.33) under a single UV excitation of 360 nm, a correlated color temperature (CCT) of 5612 K and a color rendering index (CRI) of 89. The influence of doping brought about a change in color emission, which could be substantiated by the content of different types of N configurations. As the amount of pyrrolic N decreased, the more the PL spectra shifted from blue to red, consistent with our density functional theory (DFT) calculations.

Experimental Section

Materials

P-phenylenediamine and amino acetic acid were obtained from Tianjin Guangfu Technology Development Co., Ltd. Citric acid, ethylenediamine and polymer (such as PVP) were purchased from Aladdin Technology Co., Ltd. Deionized water (18.2 MΩ cm) was used in all experiments.

Synthesis of R/G/B-CDs

A modified hydrothermal method was employed to synthesize red, green and blue emissive CDs (denoted as R-CDs, G-CDs and B-CDs). Firstly, 1 mmol of p-phenylenediamine was dissolved in 15 mL of ethanol and heated at 180 °C for 16 h to obtain the R-CDs solution. For G-CDs, 1 mmol of p-phenylenediamine was dissolved in 15 mL of water and mixed with 2 mmol of amino acetic acid and 30 μL of ethylenediamine followed by heating at 180 °C for 8 h. As for B-CDs, 1 mmol of p-phenylenediamine was dissolved in 15 mL of water and mixed with 2 mmol of citric acid solution and heated at 180 °C for 4 h. The synthesis of each CD was performed in a 25 mL Teflon-lined stainless-steel autoclave. After cooling to the room temperature, the solution was filtered by a membrane filter with a size of 0.22 μm for 24~36 h to obtain pure CDs.

Preparation of CDs/PVP composites

A measured amount of CDs is added into deionized water. Subsequently three times the amount of PVP was added into the mixture. The mixture was stirred to form a homogeneous mixture. The mixture was then put into the mould and maintained at room temperature for 4 h to cure.

Preparation of the LED devices

The mixture of CDs and PVP was dropped onto the LED chip carefully and cured at room temperature for 4 h. For the white LED, 2 mL of RGB-CDs solution with a ratio of 1:2:3.5 (B-CDs: G-CDs: R-CDs) were mixed with 2 mL of diluted water and 2.5 g of PVP, and then the mixture was shaped in the mould, covering on the LED chip (360 nm). For the blue/green/red LED, a 2 mL of B-CDs/G-CDs/R-CDs mixture was used to form the CDs/PVP discs and set onto the LED chip (360 nm).

Characterizations

Fluorescence spectroscopy was conducted using FLS980 from Techcomp (China) Ltd. to explore the time-resolved fluorescence and ultraviolet-visible (UV-Vis) absorption spectra. The morphology of the prepared CDs was investigated via transmission electron microscopy (TEM) (Model JEM-2100). A Bruker Vertex 70 V was used for the measurement of the Fourier transform infrared (FTIR) spectra. X-ray photoelectron spectroscopy (XPS) analysis was carried out by an ESCALAB 250 spectrometer with a monochromatic X-ray source Al Kα excitation (1486.6 eV). Raman spectroscopy was performed by a Horiba Jobin Yvon Xplora confocal Raman microscope with a 532 nm laser irradiation at room temperature.

Computation method

All calculations were carried out using the Gaussian 09.D01 program suite.[36] The ground state (S0) geometries of GQDs were optimized by the density functional theory (DFT) B3LYP (Becke's three-parameter hybrid function with the non-local correlation of Lee-Yang-Parr)[37] method with the Pople 6-31G(d) basis set (B3LYP/6-31G(d)). The absorption spectrum was calculated using the time-dependent DFT (TDDFT) method (at the M06-2X/6-31G(d) level) based on optimized ground state geometries. The first excited state (S1) was optimized using the TDDFT method (at the M06-2X/6-31G(d) level) to calculate the emission energy (wavelength), which corresponds to the energy difference between the ground and the first excited state. For each geometry, vibrational frequencies were calculated analytically at the same level of theory as in the previous step to ensure that it was a true local minimum.

Results and Discussion

CDs have been found to have photo physics and quantum effects, which are comparable to semiconductor QDs. CDs could also be regarded as graphitic carbon-based QDs by functionalizing with various groups. The synthesis routes of B-CDs, G-CDs and R-CDs (referred to R/G/B-CDs blow) are depicted in Figure 1(a). In this work, p-phenylenediamine was used as the precursor, which was modified by glycine via thermal solvent methods (water or ethanol). By adjusting the ratio of p-phenylenediamine and glycine, heating temperature and reaction time, the ability to control

particular emission colors of CDs was achieved. Figure 1(b-d) shows the UV-vis, PL excitation and emission spectra of the R/G/B-CDs. The prepared R-CDs, G-CDs and B-CDs had the strongest emission peaks centered at 620, 520 and 450 nm, respectively, with appropriate excitation wavelengths. Under a 365 nm UV light, the solution of R/G/B-CDs exhibited red, green and bright blue fluorescence. The QY of R-CDs was up to 24.7% after optimizing the heating time of the synthesis (Table S8). The R/G/B-CDs were all excitation-independent (Figure S1) and exhibited excellent time stability (Figure S3(a-c)), pH stability (Figure S3(d-f)), and chemical stability in 0.1 M H_2O_2 (Figure S3(g-i)) during the 30-day experimentation period. The UV-vis spectra in Figure 1(b-d) showed the absorption band at 255 nm, resulting from the π–π* transition of graphite sp2 domain. The absorption band at 300 nm was due to the n–π* transition of C → X (X = O, N) in the doped CDs. Compared with R-CDs and G-CDs, B-CDs exemplified a stronger n–π* transition, which was related to the narrow energy band. The obvious broad band at approximately 400 nm in Figure 1(c) and (d) was attributed to the trapping of excited state energy by the surface states. Especially, a red shift peak at 430 nm in R-CDs demonstrated a much broader peak than G-CDs, signifying that there existed different kinds of surface state transitions in the surface of CDs.

Figure 2(a-c) shows high dispersity of the R/G/B-CDs. The insets of high resolution TEM images exhibited very clear lattice structures of the CDs. Corresponding to the D band (1375 cm^{-1}) and G band (1580 cm^{-1}) of Raman spectra in Figure S2, the lattice fringe proved the existence of graphitic structure inside the CDs.[38-39] According to the work of Sk et al.,[40] it was reported that the luminescence wavelength of carbon-based QDs with graphene structure increases as the size increases. With the electrochemical tuning study, there exists a different theory that the luminescence wavelength is dependent on the surface of CDs rather than size.[41] The average diameter of R/G/B-CDs was approximately 2.4 ± 0.6 nm. However, there is no significant difference between three kinds of CDs in the distribution of diameters as shown in the inset of Figure 2(a-c), inferring that the size effect is not the major factor for the fluorescence color of these CDs. It is expected that the particle size distribution and surface heterogeneity have a considerable influence on the luminescence emission wavelength.

The FTIR spectra (Figure 2(d)) show the existence of the OH group (3378 cm-1) in R/G/B-CDs, corresponding to the XPS results of O 1s (Figure S4). The peaks at 1600 cm^{-1} and 1500 cm^{-1} are attributed to C=C, while the peaks at 696 cm^{-1} and 820 cm^{-1} are ascribed to the bending vibration of C=C-H. The stretching vibrations of C=N (1650 cm-1) and C-N (1230 cm-1) denoted pyridinic N and pyrrolic N, respectively, indicative of the main factor in affecting the emission colors of the CDs in this work. The content of C-N and C=N both decreased from B-CDs to R-CDs indicated pyridinic N and pyrrolic N had a significant effect on the blue shift of PL properties of CDs. Figure 2(e) shows the PL lifetimes of the three kinds of CDs, following the order of R-CDs < G-CDs < B-CDs. It is ascribed to the different chemical surface states of pyridinic N and pyrrolic N as discrete exciton trapping centres for the fluorescence emission. The detailed chemical sate analysis was evidenced by XPS spectra in Figure 2(f). The content of O in R-CDs was the lowest among three kinds of CDs (Table S2), forming the least oxygen-containing groups. Further study revealed that pyrrolic N in R-CDs was relatively low in content, while R-CDs have a higher level of C=O content rather than C-O in the structure (Table S4 and S5). As such, the results confirm that pyrrolic N structure was formed through intramolecular dehydroxylation of carboxyl groups according to the previous research.[42]

As for the XPS spectra, the peak fitting of C 1s in Figure 2(g-i) contained peaks of C=O at 289.0 eV, O=C-O at 287.8 eV, C-N /C=N at 285.9 eV, sp3 C at 284.5 eV. Figure 2(j-l) shows the high resolution XPS spectra of N 1s, comprising three species of N, including graphitic N (400.8 eV), pyrrolic N (399.6 eV) and pyridinic N (398.4 eV). The overall content of the various types of C bonds was calculated (Table S3), proving that oxidized C has a negligible effect on the red shift of CDs. Combined with Table S4, the XPS of N 1s exemplified that nearly all the N was doped in the carbon framework, causing chemical sites. In G-CDs and B-CDs, the amount of pyrrolic N and pyridinic N was fairly constant, while pyridinic N was the dominant dopant in R-CDs. Since pyrrolic N on the edge of carbon dots is a critical component of surface defect which serves as a florescence center,[43] the reduction of the amount of pyrrolic N was considered to be one of the reasons for the emission red shift of R-CDs. The content of different species of O (e.g. C=O and C-O) in the B-, G-, and R-CDs is summarized in Table S5.

We have demonstrated that the PL properties of graphene quantum dots (GQDs) can be widely tuned by their size, shape, edge structure, functional groups (Figure S9-S11), defects, and heteroatom doping. Chen et al. reported the calculated emission wavelength (nm) using the TDDFT method in a vacuum as a function of the diameter of GQDs. They also found that graphitic N doped at the edge or centre of GQDs drastically lowered the band gap, resulting in the emission of green to non-fluorescence.[40] Zbor˘il et al. synthesized red-emitting CDs; and both experimental and theoretical data confirmed that the red fluorescence stemmed from the increased amount of graphitic N in the CDs.[44] Herein, our results present that the graphitic N dopant in CDs (N-doped CDs) gave rise to an emission wavelength of > 2000 nm (Figure S9) because graphitic N centers can alter the optical properties of N-doped CDs due to the graphitic N injecting less than one excess electron into the unoccupied π* orbitals of the carbon hybrid sp2 lattice. [add_ref1] The calculations show that graphitic N doping will decrease the band gap by introducing a new mid-gap state between the HOMO and LUMO.[44-45] Based on the above information, although the XPS spectra of N 1s (Figure 2(j-l)) showed that the prepared CDs composed of

graphitic N, pyrrolic N and pyrridinic N, the fluorescence was caused by the CDs structures without graphitic N. Therefore, we have established three models containing pyrrolic N, pyrridinic N, carboxyl, epoxy, aldehyde, and sp^2 C atoms (Figure S5).

In previous study, Chen et al.[40] and Guo et al.[46] have confirmed that the emission spectrum shifted to red when hydroxyl and carboxyl were introduced into GQDs either in the plane or at the edge. In this work, the GQD models showed different fluorescence characteristics, corresponding to blue-green-red emissions from the different types and magnitude of radicals. The effects of various functional groups on the emission spectrum, including amino, imino, epoxy, aldehyde, ester, and C=O are presented in the Electronic Supplementary Information (Figure S9-S11). The XPS and FTIR spectra also show that there were different kinds of functional groups/radicals, and the N-dopant on the prepared R/G/B-CDs, which emitted blue, green and red fluorescence (shown as Figure S5) was due to the combination of different effects of radicals on the fluorescence emission. Thus, by adjusting the number and types of functional groups attached on GQDs, we can ultimately change the emission wavelength, thereby obtaining the desired fluorescence properties.

Figure 3(a-c) shows the optical micrographs of R/G/B-CDs/PVP composite discs covering on the LED devices with a wavelength of 360 nm. Due to the high dispersity of R/G/B-CDs within PVP, the R/G/B-CDs/PVP composite discs emitted bright blue, green and red fluorescence under the excitation of LED devices, which was similar to the solution. The CIE color coordinates of the R/G/B-CDs solution are shown in (Figure S7), which are (0.18, 0.16), (0.31, 0.54) and (0.63, 0.37), respectively.

The fluorescence emission spectra of the as-prepared CDs demonstrate little peak shift in different solvents (Figure S6). The R/G/B-CDs@PVP discs were transparent and exhibited uniform multiple color emissions from blue to red under the same excitation wavelength (360 nm). The QY of the R/G/B-CDs@PVP composites in Table S7 are 6.5%, 21.1% and 14.6%, respectively. The Different ratios of three kinds of R/G/B-CDs were mixed together into the PVP sol-gel solution to determine the appropriate proportion to develop white LED. The PL spectra of CDs/PVP composites manifested a wide lighting band covering the whole visible light range at excitation of 340 and 360 nm, which is exactly what white LED devices need (Figure 3(e)). After performing different ratios of the R/G/B-CDs@PVP composites (Figure S8 and Table S6), the final CIE color coordinates of the white LEDs were (0.33, 0.33), which were akin to natural sunlight (Figure 3(d)). The CCT of the white LEDs was 5612 K and a CRI was 89. After a 15-day irradiation with ultraviolet light, the PL spectrum of white LED retained a good luminescence without much photobleaching. The temperature-dependent PL spectra (Figure S13) showed the good thermal stability of the white LED. This signifies that the R/G/B-CDs-based white LED device endowed excellent stability. Therefore, these results further prove the ability of the R/G/B-CDs to be employed as potential phosphors for white LEDs.

Conclusions

The monomer p-phenylenediamine was used for its cyclization effect with different modifying agents (e.g. amino acetic acid) to synthesize R/G/B-CDs using a facile one-pot solvothermal method. The QY of the R-CDs recorded 18.8%. A good dispersity of the prepared CDs in PVP was achieved, and the composites were further used for the design of LEDs, including a white LED with a CIE coordinate of (0.33, 0.33) under a single UV excitation of 360 nm with remarkable anti-photobleaching and a CRI of 89. Fascinatingly, this novel type of white LEDs is less detrimental to the retina compared to the blue light excitation based white LEDs. Apart from the experimental results, a systematic exploration of the effects brought by N-doping has been corroborated by a DFT computation approach. As such, the results unveil a controllable design for the PL properties of CDs through adjusting the amount and types of functional groups, which can promote the advancement of nanoscience and nanotechnology.

Conflicts of interest

There are no conflicts to declare.

Acknowledgements

The acknowledgements come at the end of an article after the conclusions and before the notes and references. We thank Beijing Nova Program Interdisciplinary Studies Cooperative project (No. Z181100006218138), Science Foundation of China University of Petroleum-Beijing (No. 2462018BJC004), National Institute of Food and Agriculture, U.S. Department of Agriculture, and McIntire Stennis under accession number 1009735 for the support. W.-J. Ong acknowledges financial assistance and faculty start-up grants and supports from Xiamen University.

Notes and references

1 Xu, Q.; Kuang, T.; Liu, Y.; Cai, L.; Peng, X.; Sreenivasan Sreeprasad, T.; Zhao, P.; Yu, Z.; Li, N., *J. Mater. Chem. B* 2016, ***4***, 7204.

2 Ong, W.-J.; Tan, L.-L.; Ng, Y. H.; Yong, S.-T.; Chai, S.-P., *Chem. Rev.* 2016, ***116***, 7159.

3 Chao, D.; Zhu, C.; Xia, X.; Liu, J.; Zhang, X.; Wang, J.; Liang, P.; Lin, J.; Zhang, H.; Shen, Z. X.; Fan, H. J. *Nano Lett.*, 2015, ***15***, 565.

4 Wang, H.; Wang, L.; Chen, S.; Li, G.; Quan, J.; Xu, E.; Song, L.; Jiang, Y., *J. Mater. Chem. A* 2017, ***5***, 3569.

5 Ananthanarayanan, A.; Wang, X.; Routh, P.; Sana, B.; Lim, S.; Kim, D. H.; Lim, K. H.; Li, J.; Chen, P., *Adv. Funct. Mater* 2014, ***24***, 3021.

6 Li, X.; Rui, M.; Song, J.; Shen, Z.; Zeng, H., *Adv. Funct. Mater* 2015, ***25***, 4929.
7 Lim, S. Y.; Shen, W.; Gao, Z., *Chem. Soc. Rev*.2015, ***44***, 362.
8 Xiao, L.; Sun, H., *Nanoscale Horiz.* 2018, ***3***, 565.
9 Tong, G.; Li, H.; Li, D.; Zhu, Z.; Xu, E.; Li, G.; Yu, L.; Xu, J.; Jiang, Y., *Small* 2018, ***14***, 1702523.
10 Citterio, D.; Minamihashi, K.; Kuniyoshi, Y.; Hisamoto, H.; Sasaki, S.-i.; Suzuki, K., *Anal. Chem.* 2001, ***73***, 5339.
11 Zhang, T.; Zhao, F.; Li, L.; Qi, B.; Zhu, D.; Lü, J.; Lü, C., *ACS Appl. Mater. Interface* 2018, ***10***, 19796.
12 Zou, Y.; Liu, Y.; Ban, M.; Huang, Q.; Sun, T.; Zhang, Q.; Song, T.; Sun, B., *Nanoscale Horiz.*2017, ***2***, 156.
13 Jiang, Y.; Cho, S.-Y.; Shim, M., *J. Mater. Chem. A* 2018, ***6***, 2618.
14 Xu, Q.; Li, W.; Ding, L.; Yang, W.; Xiao, H., Ong, W., Nanoscale 2019, doi: 10.1039/c8nr08738e
15 Sarkar, S.; Sudolská, M.; Dubecky, M.; Reckmeier, C.; Rogach, A.; Zboril, R.; Otyepka, M., J. Phys. Chem. C2016, 120, 1303-1308.
16 Chang, Y.; Yao, X.; Zhang, Z.; Jiang, D.; Yu, Y.; Mi, L.; Wang, H.; Li, G.; Yu, D.; Jiang, Y., 2015, ***3***, 2831.
17 Bhunia, S. K.; Saha, A.; Maity, A. R.; Ray, S. C.; Jana, N. R., *Sci. Rep.*2013, ***3***, 1473.
18 Ding, H.; Yu, S.-B.; Wei, J.-S.; Xiong, H.-M., *ACS Nano*. 2016, ***10***, 484.
19 Songnan, Q.; Ding, Z.; Di, L.; Wenyu, J.; Pengtao, J.; Dong, H.; Lei, L.; Haibo, Z.; Dezhen, S., *Adv. Mater.*2016, ***28***, 3516.
20 Dan, Q.; Zaicheng, S.; Min, Z.; Jing, L.; Yongqiang, Z.; Guoqiang, Z.; Haifeng, Z.; Xingyuan, L.; Zhigang, X., *Adv. Opt. Mater.*2015, ***3***, 360.
21 Shamsipur, M.; Barati, A.; Karami, S., *Carbon*, 2017, ***124***, 429.
22 Miao, X.; Qu, D.; Yang, D.; Nie, B.; Zhao, Y.; Fan, H.; Sun, Z., *Adv. Mater.,* 2018, ***30***, 1704740.
23 Yuan, F.; Yuan, T.; Sui, L.; Wang, Z.; Xi, Z.; Li, Y.; Li, X.; Fan, L.; Tan, Z. a.; Chen, A.; Jin, M.; Yang, S., *Nat. Commun*., 2018, ***9***, 2249.
24 Zhen, T.; Xutao, Z.; Di, L.; Ding, Z.; Pengtao, J.; Dezhen, S.; Songnan, Q.; Radek, Z.; L., R. A., *Adv. Opt. Mater* 2017, ***5***, 1700416.
25 Xu, J.; Miao, Y.; Zheng, J.; Wang, H.; Yang, Y.; Liu, X., *Nanoscale*, 2018, ***10***, 11211.
26 Kim, D. H.; Kim, T. W., N*ano. Energ.,* 2017, ***32***, 441.
27 Lu, S.; Sui, L.; Liu, J.; Zhu, S.; Chen, A.; Jin, M.; Yang, B., *Adv. Mater.,*2017, ***29***, 1603443.
28 Lougheed, T., *Environ. Health Perspect.* 2014, ***122***, A81.
29 R., W. A.; E., R. J., *Photochem. Phoobiol.* 2012, ***88***, 1320.
30 Xu, Q.; Pu, P.; Zhao, J.; Dong, C.; Gao, C.; Chen, Y.; Chen, J.; Liu, Y.; Zhou, H., *J. Mater. Chem. A.*, 2015, ***3***, 542.
31 Xu, Q.; Liu, Y.; Su, R.; Cai, L.; Li, B.; Zhang, Y.; Zhang, L.; Wang, Y.; Wang, Y.; Li, N., *Nanoscale*. 2016, ***8***, 17919.
32 Xu, Q.; Liu, Y.; Gao, C.; Wei, J.; Zhou, H.; Chen, Y.; Dong, C.; Sreeprasad, T. S.; Li, N.; Xia, Z., *J. Mater. Chem. C.*2015, ***3***, 9885.
33 Xu, Q.; Ding, L.; Wen, Y.; Yang, W.; Zhou, H.; Chen, X.; Street, J.; Zhou, A.; Ong, W.-J.; Li, N., *ACS Appl. Mater. Interface* 2018, ***6***, 6360.
34 Xu, Q.; Su, R.; Chen, Y.; Theruvakkattil Sreenivasan, S.; Li, N.; Zheng, X.; Zhu, J.; Pan, H.; Li, W.; Xu, C.; Xia, Z.; Dai, L., *ACS Appl. Nano Mater.* 2018, ***1***, 1886.
35 Xu, Q.; Li, B.; Ye, Y.; Cai, W.; Li, W.; Yang, C.; Chen, Y.; Xu, M.; Li, N.; Zheng, X.; Street, J.; Luo, Y.; Cai, L.,*Nano Res*. 2018, ***11***, 3691.
36 Frisch, M. J.; Trucks, G.; Schlegel, H. B.; Scuseria, G.; Robb, M.; Cheeseman, J.; Scalmani, G.; Barone, V.; Mennucci, B.; Petersson, G.,. *Gaussian Inc. Wallingford CT* 2009, ***27***, 34.
37 Becke, A. D., *J. Chem. Phys.* 1993, ***98***, 5648.
38 Ferrari, A. C.; Robertson, J., *Phys. Rev. B* 2000, ***61***, 14095.
39 Zhang, M.; Su, R.; Zhong, J.; Fei, L.; Cai, W., Guan, Q.; Li, W.; Li, N.; Chen, Y.; Cai, L.; Xu, Q., Nano Res, 10.1007/s12274-019-2293-z.
40 Sk, M. A.; Ananthanarayanan, A.; Huang, L.; Lim, K. H.; Chen, P., *J. Mater. Chem. C*2014, ***2***, 6954.
41 Bao, L.; Zhang, Z.-L.; Tian, Z.-Q.; Zhang, L.; Liu, C.; Lin, Y.; Qi, B.; Pang, D.-W., *Adv. Mater.* 2011, ***23***, 5801.
42 Qu, D.; Zheng, M.; Zhang, L.; Zhao, H.; Xie, Z.; Jing, X.; Haddad, R. E.; Fan, H.; Sun, Z., *Sci. Rep*. 2014, ***4***, 5294.
43 Dong, Y.; Pang, H.; Yang, H. B.; Guo, C.; Shao, J.; Chi, Y.; Li, C. M.; Yu, T., *Angew. Chem. Int. Ed.* 2013, ***125***, 7954.
44 Holá, K.; Sudolská, M.; Kalytchuk, S.; Nachtigallová, D.; Rogach, A. L.; Otyepka, M.; Zbořil, R., *ACS Nano.* 2017, ***11***, 12402.
45 Sarkar, S.; Sudolská, M.; Dubecký, M.; Reckmeier, C. J.; Rogach, A. L.; Zbořil, R.; Otyepka, M., *J. Phys. Chem. C* 2016, ***120***, 1303.
46 Meilian, Z.; Feng, Y.; Ying, X.; Dan, X.; Yong, G., *Chem. Phys. Chem.* 2014, ***15***, 950.

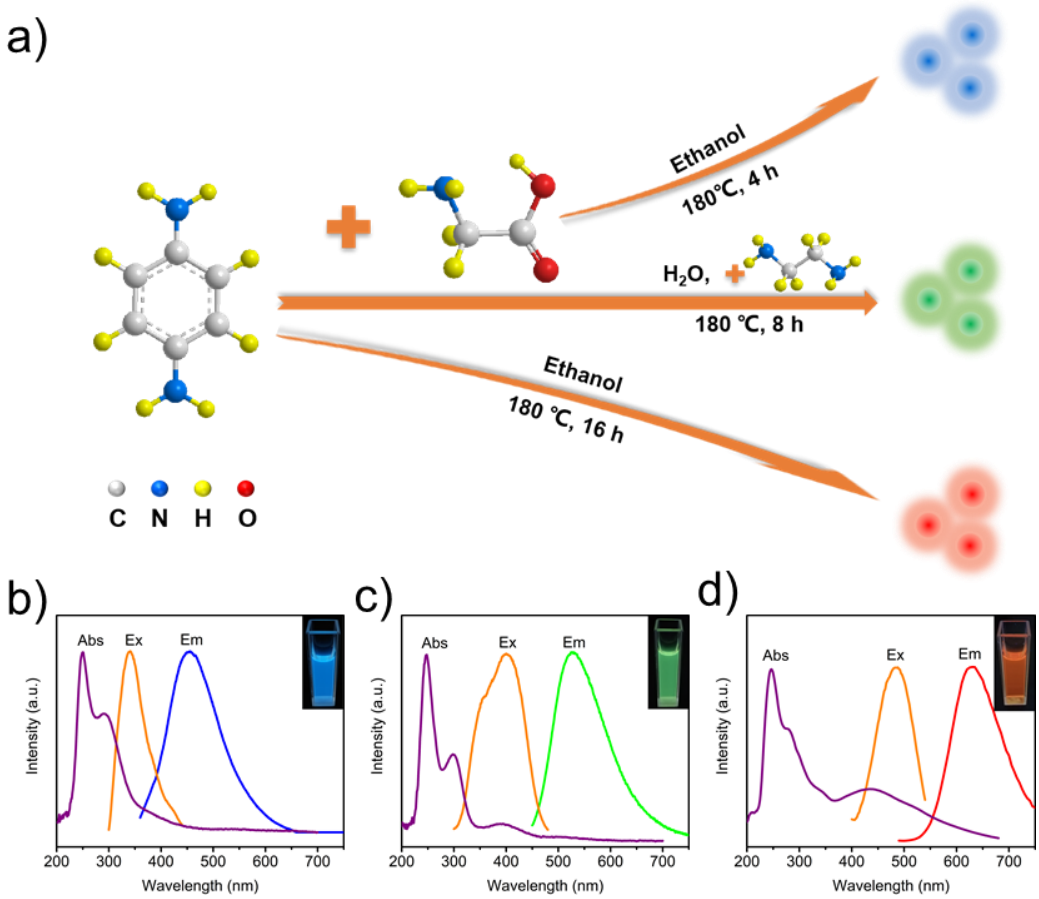

Figure 1. (a) Schematic of the synthesis of R/G/B-CDs with red, green and blue luminescence (excited by UV-light at 365 nm). (b-d) The corresponding UV–vis, PL emission, and PL excitation spectra with a normalization of (b) B-CDs, (c) G-CDs and (d) R-CDs. Insets of (b)-(d) show the digital photos of R/G/B-CDs under UV light at 365 nm.

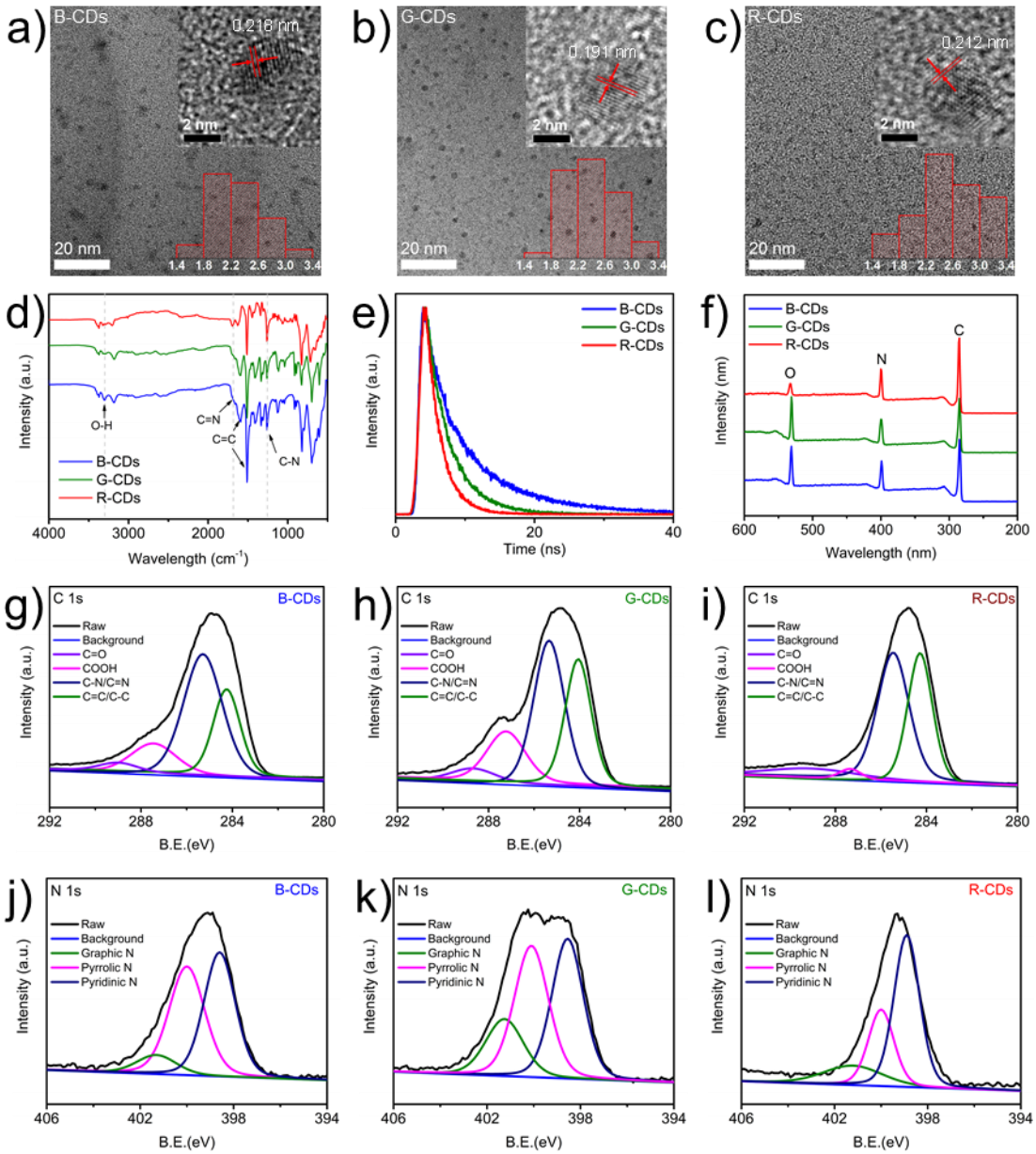

Figure 2. (a-c) TEM images of R/G/B-CDs (insets are corresponding high resolution TEM images at top right corner and the diameter distributions at the bottom right corner). (d) FTIR spectra and (e) PL lifetimes of R/G/B-CDs under 365 nm impulse excitation. (f) The XPS survey spectra of the R/G/B-CDs. High resolution XPS spectra of (g-i) C 1s and (j-l) N 1s of R/G/B-CDs.

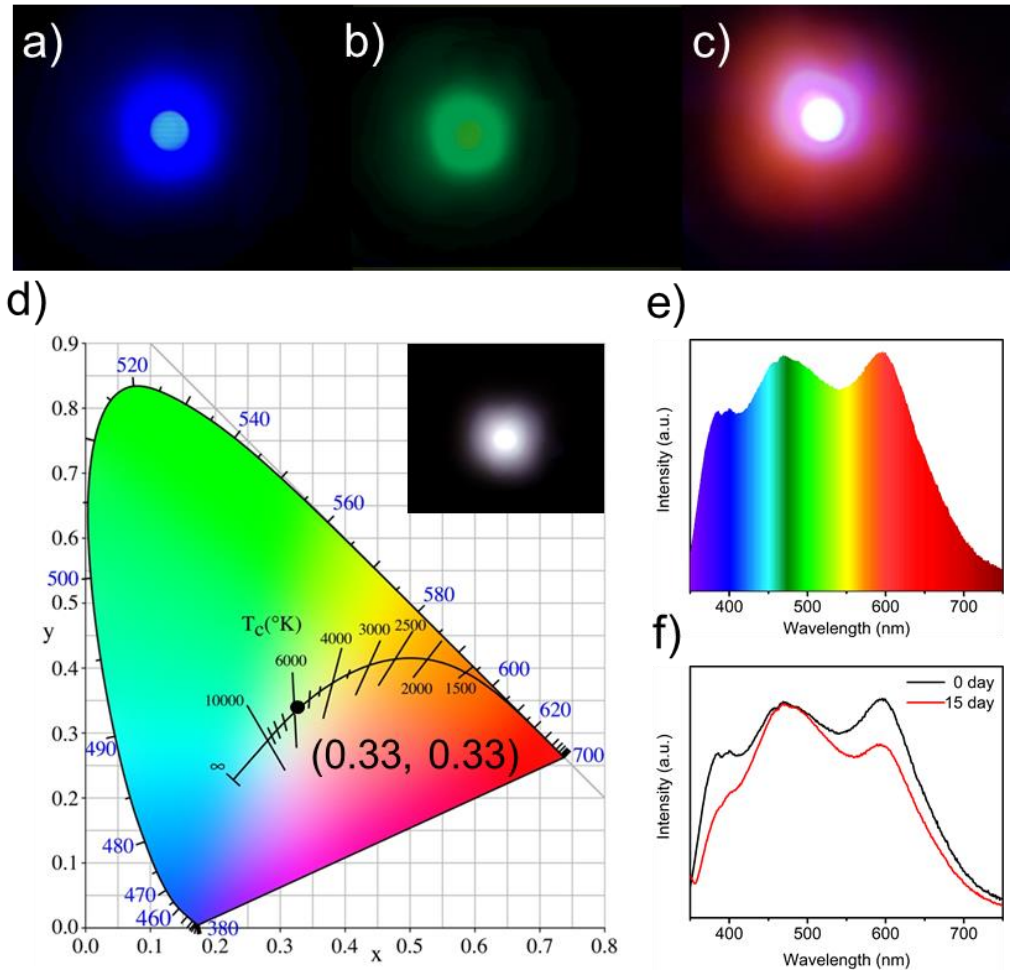

Figure 3. (a-c) The photographs of the monochrome blue, green and red down-conversion LED devices from coating CDs/PVP on the chips under the same excitation. (d) The CIE color coordinates of the white LEDs. Inset shows the photo of the white light upon excitation. (e) The emitting light spectrum of white LEDs. (f) The emitting spectra of the white LED before and after 15 days.